

S & M 0696

Microneedle System for Localized Drug Injection Using Embedded Microfluid Source

Jae-won Ban, Kyo-in Koo, Sunkil Park, Gilsub Kim,
Doyoung Jeon¹ and Dong-il “Dan” Cho*

ASRI / ISRC / NB&SRC, School of Electrical Engineering and Computer Science,
Seoul National University, 599 Gwanangno, Gwanak-gu, Seoul 151-742, Korea

¹Department of Mechanical Engineering, Sogang University,
Shinsudong, Mapoku, Seoul 121-742, Korea

(Received May 8, 2007; accepted September 7, 2007)

Key words: microneedle, drug injection, microfluid source, azobisisobutyronitrile (AIBN), microheater

In this paper, we present a novel microneedle system for injecting drugs using an embedded microfluid source. This microneedle system consists of in-plane microneedles, a drug reservoir, a chemical fluid source, a chemical fluid source chamber, and a microheater. The microneedles, drug reservoir, and chemical fluid source chamber are connected by microchannels. The chemical fluid source, azobisisobutyronitrile (AIBN) decomposes and produces nitrogen gas and a free radical at approximately 70° C. Using this phenomenon, the AIBN on the microheater generates nitrogen gas upon the application of electrical power, and then the generated gas injects the drug in the drug reservoir through the microchannels to the microneedles. This system can inject 2.29–2.9 μl blue ink in approximately 6 s at a voltage and current of 30.4 V and 164 mA, respectively, using 5 μl AIBN. This novel microneedle system is expected to be applicable to highly precise biological experiments.

1. Introduction

Advances in micromachining technology have resulted in the development of many biomedical instruments, including microneedles, micropumps, lab-on-a-chip devices, and microelectrodes. A microsize drug injection system is expected to have many advantages in terms of minimal invasiveness, precise penetration depth control, nanoliter-range drug volume control, and highly localized drug delivery. In spite of these advantages, no microsize drug delivery system has yet been reported. One of the principal reasons

*Corresponding author: e-mail: dicho@snu.ac.kr

for this is the difficulty of integrating a microneedle and a micropump. Although these two major components have already been developed separately,⁽¹⁻¹²⁾ the developed components are difficult to fabricate in the same substrate.

Our research team has reported the fabrication of in-plane microneedles.^(1,2,4) The microchannel of the developed microneedles was fabricated parallel to the substrate surface so that it could easily be connected to other areas in the processing substrate. Therefore, the microneedles were easily integrated with drug reservoirs and microelectrodes.^(1,2)

Azobisisobutyronitrile (AIBN) decomposes and produces nitrogen gas and a free radical at approximately 70°C.⁽¹²⁻¹⁴⁾ Using this property, AIBN on a simple microheater can function as a fluidic power source.⁽¹²⁾ By a simple modification of the gas outlet, this fluidic power source can be integrated with in-plane microneedles.

In this paper, we present a novel microneedle system for localized drug injection using embedded AIBN. In-plane microneedles are fabricated with the drug reservoir and the AIBN chamber in the same Si substrate in a single batch process. The microheater is fabricated on Pyrex glass, and the AIBN is screen-printed on the fabricated microheater. The integration process is performed by bonding the Si part to the glass part using polydimethylsiloxane (PDMS). The AIBN on the microheater generates nitrogen gas upon heating, and then the generated gas injects the drug in the drug reservoir through the microchannels to the microneedles.

2. Design

The proposed system consists of four parts: three microneedles, a drug reservoir, an AIBN chamber, and a microheater used for igniting the AIBN (Fig. 1(a)). The microneedles, drug reservoir, and AIBN chamber are connected with microchannels in the Si substrate. The microheater is located on the Pyrex glass substrate. The glass substrate containing the microheater and the AIBN chamber in the Si substrate form an enclosed space by the PDMS bonding process. When electric power is used to heat the AIBN through the microheater, the decomposed nitrogen gas induces the drug from the drug reservoir to the microneedles through the microchannels, as shown in Fig. 1(b).

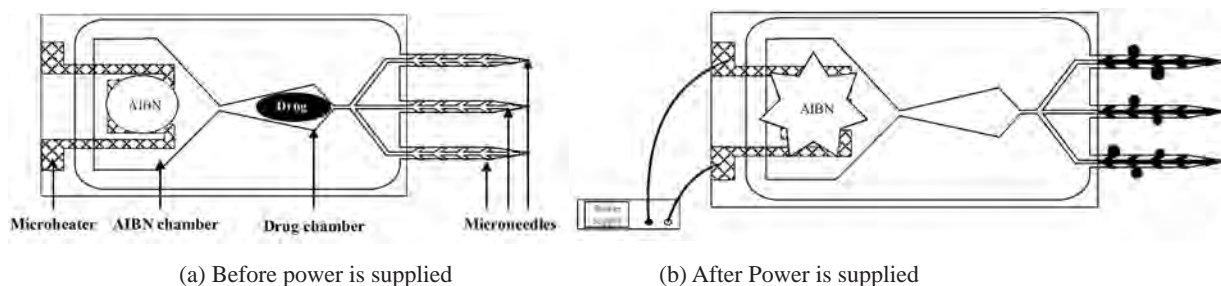


Fig. 1. Microneedle system injection concept.

2.1 Fluid source

Some solid chemical propellants simply require thermal energy for gas generation; thus, they are widely applied in the propulsion of microspacecraft in space. However, space-applicable propellants must function at high operating temperatures of over 400°C and release nitrogen gas with toxic by-products such as CO and C_xH_y .⁽¹⁵⁾ However, AIBN decomposes and produces inert nitrogen gas and a free radical at approximately 70°C, as shown in Fig. 2.⁽¹²⁻¹⁴⁾ The decomposition temperature of AIBN is relatively low; thus, the system operates with low electricity consumption. To keep the AIBN powder (Unisource, India) on the microheater in an environment subject to shocks or vibration, it is mixed with Teflon® (Teflon® AF 2400, DuPont Korea, Korea), and is used in solid-matrix form.⁽¹²⁾ Thus, the AIBN powder is not expected to react with the stored drug in the drug reservoir of the microneedle system during the injection process. The low decomposition temperature makes AIBN highly applicable to this microneedle system.

2.2 Microheater design

A thin film gold / titanium microheater is designed and fabricated for the AIBN ignition. To ignite the AIBN, a microheater must reach a temperature of over 70°C. It is designed to have a length of 151.2 mm, a width of 100 μm, and a thickness of 4000 Å, as shown in Fig. 3. The resistivity of Au thin film at 300 K is $3.99 \times 10^{-8} \Omega \cdot m$ according to Matthiessen's Rule.⁽¹⁶⁾ Therefore, the resistance of the thin-film microheater is calculated to be 148.75 Ω. The measured value of the resistance is 161 Ω. The error is suspected

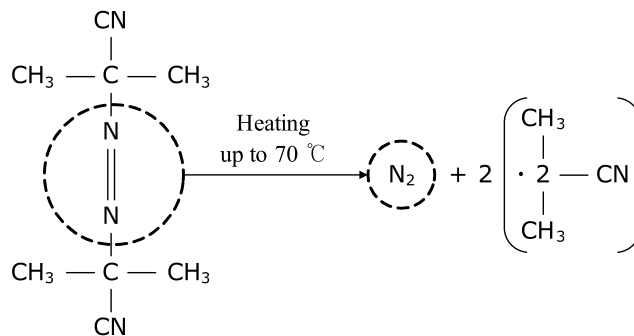


Fig. 2. AIBN decomposition mechanism.⁽¹²⁻¹⁴⁾

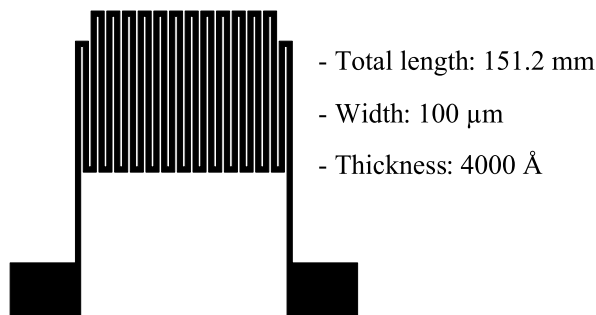


Fig. 3. Microheater design.

to originate from the 500 Å Ti adhesion layer. The microheater reaches 70°C when electrical power of 0.5 W is supplied.

2.3 Microneedle and microchannel design

In our previous study, the D-type microneedle shank in Table 1 showed the most stable mechanical properties.⁽¹⁾ The microneedle shank fabricated with the D-type design has an average bending load of 124 mN, an average buckling force of 6.28 N, and an average penetration force of 80.9 mN. These microneedles were used without breakage for the extraction of samples from the small intestines of an anesthetized pig and for drug delivery into a rat brain using a macropump.^(4,17) On the basis of these experimental results, a D-type microneedle shank was chosen with a length of 2 mm, a width of 200 µm, and a thickness of 100 µm.

For the same injected volume, lower flow resistance in the microchannels enables a lower volume of AIBN to be used. To realize lower flow resistance, the fluid flow in the microchannels is simulated using FEMLAB™ 3.2 (Comsol, U.S.A.). In the simulation, the fluid flow is assumed to be laminar. Table 2 shows the results of the microchannel simulation. When the number of outlets decreases, the channel becomes narrower, or the number of needles decreases, the flow velocity is predicted to increase. From the simulation results, a microchannel is chosen with 11 outlets and a width of 20 µm. The shape of the drug reservoir is also simulated to minimize turbulence flow. Lower turbulence flow enables less wastage of fluid power during the transfer in the drug reservoir. A rhombus-shaped drug reservoir was shown to have the highest fluid velocity and the lowest turbulence flow, as shown in Fig. 4.

3. Fabrication

The device fabrication process can be divided into three main parts: a Si process for the microneedles and microchannels, a glass process for the microheater and AIBN matrix screen-printing, and a bonding process using PDMS.

Table 1
Various designs of microneedle shanks.⁽¹⁾




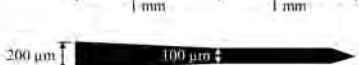
Type	Overall geometry	Shape of the tip	Tip taper angle (°)
A		Right triangle	8.5
B		Right triangle	15
C		Isosceles triangle	9.5
D		Isosceles triangle	30

Table 2

Simulation of microfluidic flow under various conditions using FEMLABTM 3.2 with the input velocity of 0.2 m/s.

Condition	Value	Velocity (Needle tip)	Pressure (Chamber)
Length of shank	2 mm	52.7 mm/s	1.3×10^5 Pa
	4 mm	52.7 mm/s	1.6×10^5 Pa
Number of outlets	1	25.7 mm/s	1.1×10^5 Pa
	5	2 – 25.7 mm/s	1.0×10^5 Pa
	11	0 – 25.7 mm/s	1.0×10^5 Pa
Width of channel	20 μm	52.7 mm/s	2.7×10^5 Pa
	40 μm	25 mm/s	1.3×10^5 Pa
	60 μm	10 mm/s	1.0×10^5 Pa
Number of needles	1	25 mm/s	1.0×10^5 Pa
	3	22 mm/s	1.0×10^5 Pa

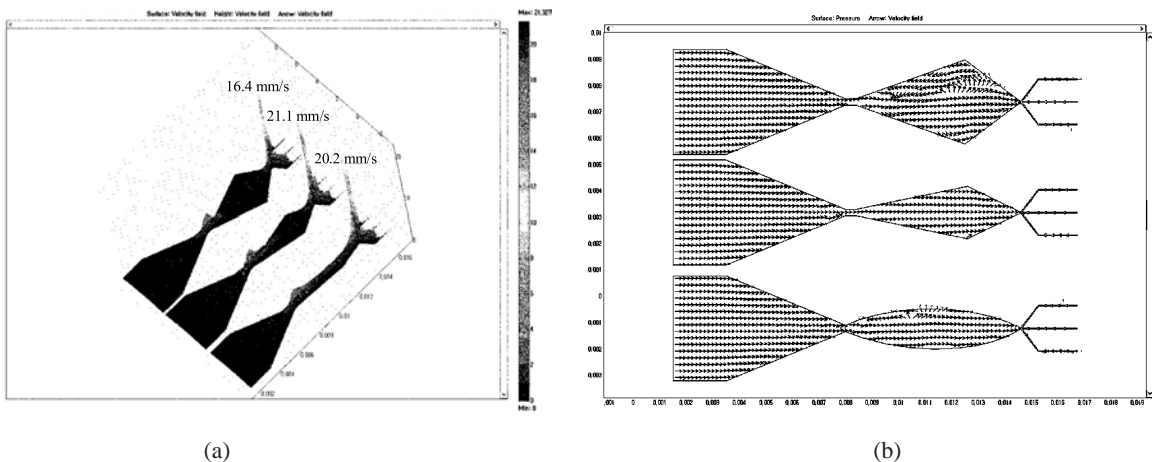


Fig. 4. Simulation results. (a) Fluid velocity for each chamber shape. (b) Fluid flow direction for each chamber shape.

3.1 *Si part fabrication*

Figure 5 shows the Si process. The anisotropic dry-etching step defines the depth of the buried microchannels. Then, isotropic dry etching defines the diameter of the microchannels. Polysilicon deposition by low pressure chemical vapor deposition (LPCVD) is performed to refill the trenches formed by anisotropic etching, thus completing the microchannel formation.^(1,2,18–20) The dry-etching step can be performed in any direction on the wafer; hence, the direction of microchannels can be designed freely, in contrast with channel formation by wet etching.⁽²¹⁾ In our previous work, the trenches were parallel to the direction of the microchannels; thus, the microchannels were semicircular and their area was restricted, as shown in Fig. 6(a).⁽⁴⁾ In this work, the trenches are perpendicular to the direction of the microchannels; thus, the microchannels

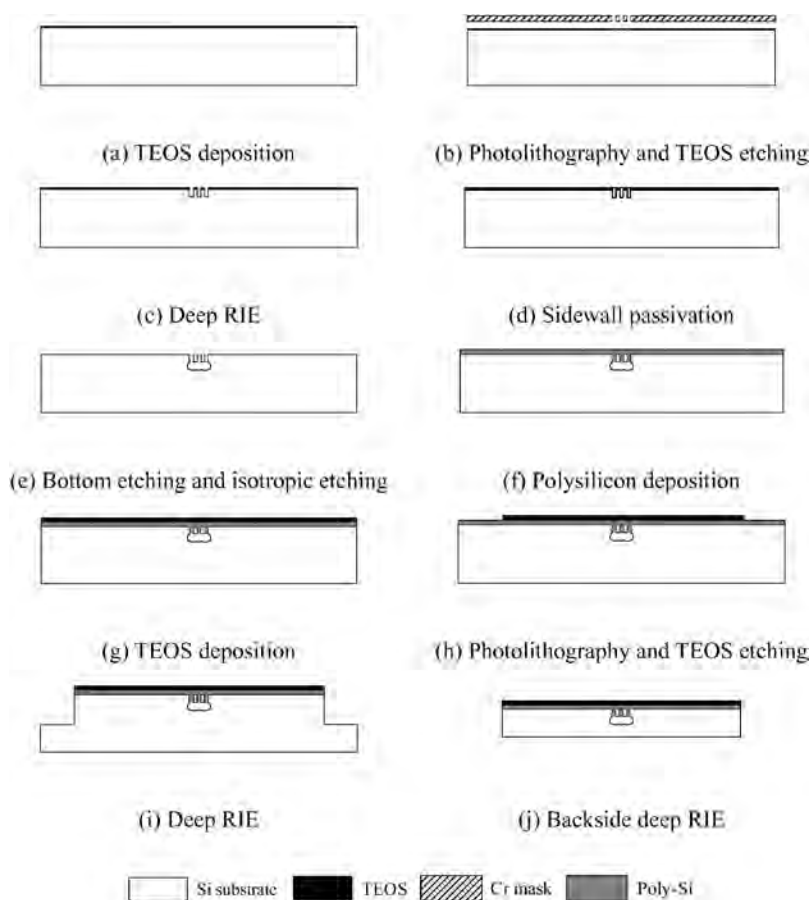


Fig. 5. Process flow of microneedle fabrication.

are semielliptical and their area is larger than that in our previous work, as shown in Fig. 6(b). After channel formation, two anisotropic dry-etching steps were performed to define and release the Si substrate. The drug reservoir and the AIBN chamber were also fabricated in this process. The fabricated Si part has a drug inlet to supply the drug to the drug reservoir (Fig. 7).

3.2 Microheater fabrication

Figure 8 shows the glass process. The microheater used for the AIBN ignition is fabricated by patterning a 500-Å-thick titanium film and a 4000-Å-thick gold film on a 350-µm-thick Pyrex-7740 glass wafer. The glass wafer is selected as the process substrate for the microheater because of its lower thermal conductivity and higher electrical resistivity than those of a Si wafer.⁽²²⁾ Titanium is used as an adhesion layer

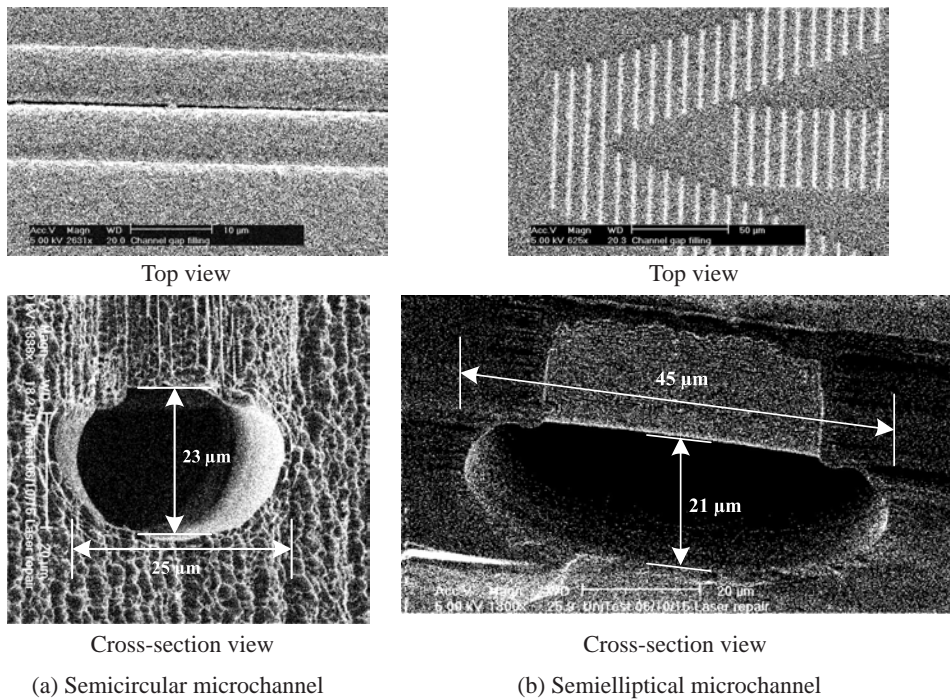


Fig. 6. SEM images of microchannels.

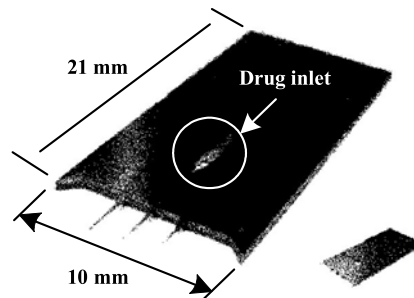


Fig. 7. Fabricated Si part.

to improve the adhesive strength between the Pyrex glass and the gold film. Figure 9 shows the temperature change in the fabricated microheater as the DC voltage changes. The microheater is heated to 70°C by applying a voltage of 9 V and a current of 56 mA.

3.3 Bonding process

Figure 10 shows the bonding process. PDMS (Sylgard 184, Dow Corning Co., MI, U.S.A.) is used to form the AIBN chamber shape on the glass part by soft lithography after the deposition of a layer of PMER (PMER N-D40SY, OHKA, Japan). Figure 11(a) shows the fabricated glass part with the patterned PDMS on the microheater substrate. Pure AIBN powder (Unisource, India) is mixed with Teflon® powder (Teflon® AF 2400,

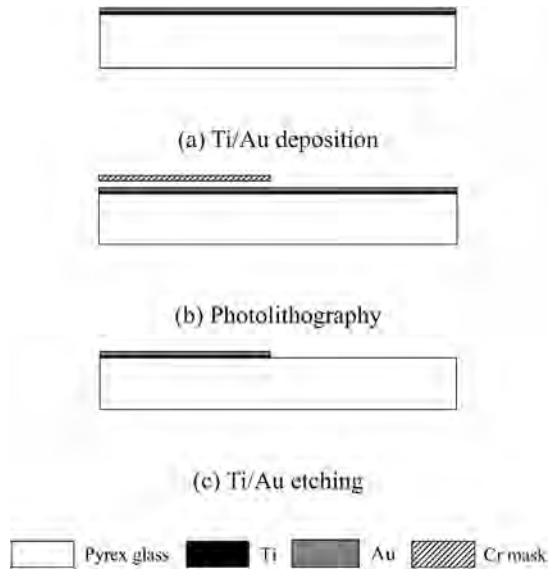


Fig. 8. Process flow of microheater fabrication.

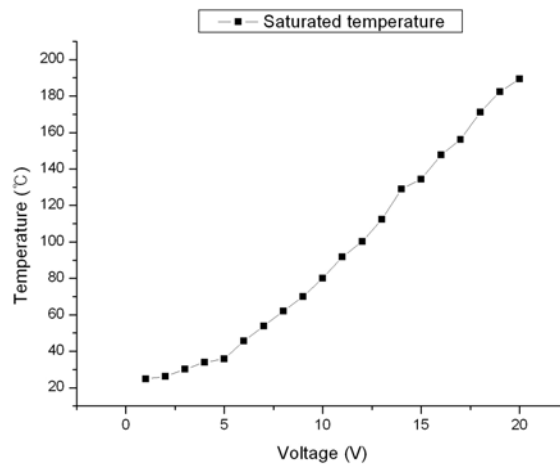


Fig. 9. Measured microheater temperature with respect to voltage.

DuPont Korea, Korea) at a ratio of 3:1 in a solvent (PF-5080, 3M Korea, Korea).^(12,23) The AIBN matrix sol-gel is then screen-printed on the microheater and cured at room temperature. The PDMS on the glass part is surface-treated using a high-voltage spark, the effect of which is similar to that of O₂ plasma treatment. Immediately after the

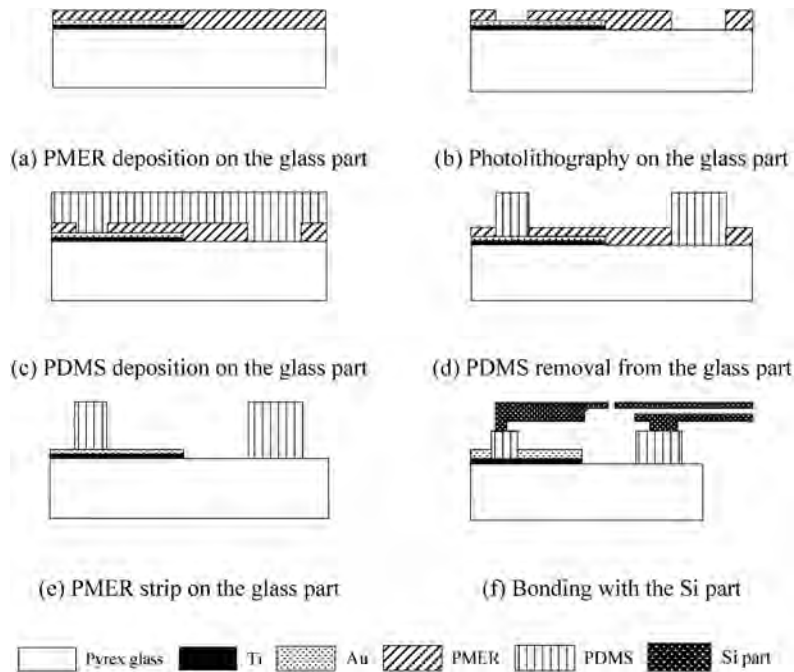


Fig. 10. Bonding process flow.

surface treatment, the Si part is bonded with the glass part. Figure 11(b) shows the bonded microneedle system.

4. Experiments and Discussion

To verify the nonclogging of the microchannels, an experiment is performed, the configuration of which is shown in Fig. 12. In this setup, only the Si part without the glass part is connected to a syringe pump. Blue ink in the drug reservoir is ejected through the microneedles using the syringe pump. This test shows that the microchannels do not become clogged.

The drug injection test of the whole system is performed by connecting the microheater to the electrical power source, as shown in Fig. 13(a). Before setting up this configuration, blue ink is supplied to the drug reservoir through the inlet of the Si part, and then the inlet is covered and fixed using glue. 5 μl of AIBN is screen-printed in this experiment. A voltage of 30.4 V and a current of 164 mA are applied, as shown in Fig. 13(a). After 2 s, the AIBN releases nitrogen gas, and the system injects the blue ink in the drug reservoir through the microneedles. 2.29–2.9 μl of ink is injected in approximately 6 s, as shown in Fig. 13(b). This value is calculated by analyzing moving

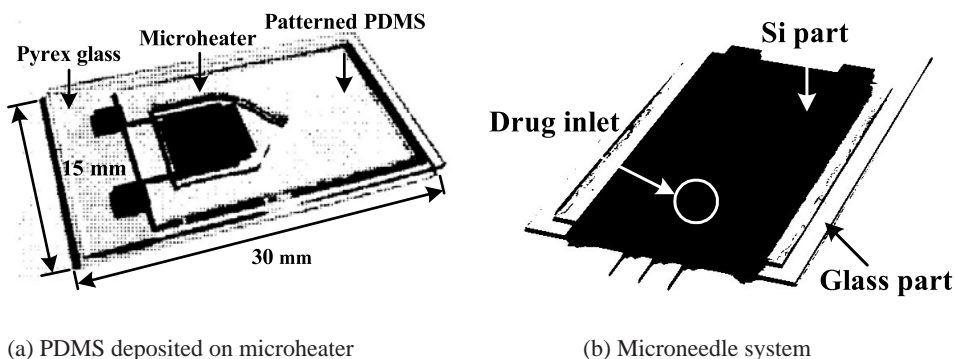


Fig. 11. Fabrication results.

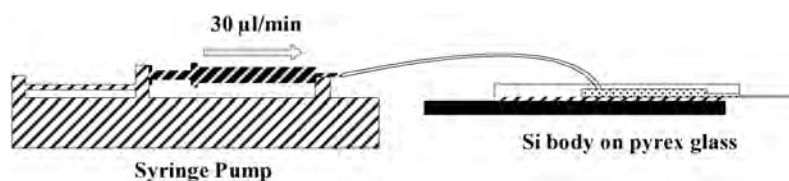


Fig. 12. Microchannel formation test.

pictures of the experiment. The AIBN ignites at 30.4 V, which is larger than the expected voltage. It is suspected that the heat from the microheater is transferred not only to the AIBN, but also to the Pyrex glass and the PDMS.

5. Conclusions

A novel microneedle system for localized drug injection was developed. The developed system consisted of microneedles integrated with a simple microsize chemical pump instead of a complex microsize mechanical pump. The microneedles of this system are made of Si and have good mechanical stability, as shown in previous research. This system can inject 2.29–2.9 μl blue ink in approximately 6 s at a voltage and current of 30.4 V and 164 mA, respectively. The power consumed by the system is expected to decrease upon using a lower-thermal-conductivity substrate. Because of the limitations of the microfluid analysis tool, the actual performance of this system cannot easily be estimated by simulation. The developed system can be applicable to highly precise biological experiments such as cell, neuron, and brain experiments. In addition, this system can also be used as a disposable drug injector with minimal invasiveness for patients with chronic diseases.

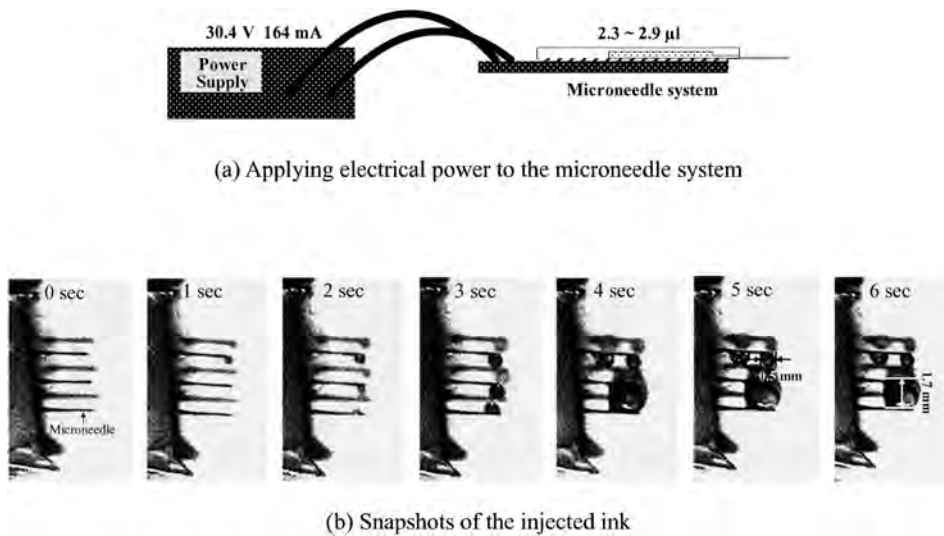


Fig. 13. Drug injection test using the microneedle system.

Acknowledgements

This research has been supported by the Intelligent Microsystem Center (IMC; <http://www.micro-system.re.kr>), as a 21st Century Frontier R&D Project sponsored by the Korea Ministry of Commerce, Industry and Energy, by a grant from the Korea Health 21 R&D Project, Ministry of Health & Welfare, Republic of Korea (A05-0252-B20604-05N1-00010A), and by the SRC/ERC program of MOST/ KOSEF (grant # R11-2000-075-01001-0).

References

- 1 S. J. Paik, S. W. Byun, J. M. Lim, Y. H. Park, A. R. Lee, S. Chung, J. K. Chang, K. J. Chun and D. I. Cho: *Sens. Actuators A* **114** (2004) 276.
- 2 K. I. Koo, J. M. Lim, S. J. Paik, J. H. Park, S. W. Byun, A. R. Lee, S. G. Park, T. Y. Song, H. M. Choi, M. J. Jeong and D. I. Cho: *Sens. Mater.* **17** (2005) 87.
- 3 P. A. Stupar and A. P. Pisano: *Proc. Transducers '01: Tech. Dig. 11th Int. Conf. Solid State Sensors and Actuators (Munich, 2001)* p. 1386.
- 4 S. J. Paik, A. R. Lee, K. I. Koo, S. K. Park, M. J. Jeong, H. M. Choi, J. M. Lim, S. J. Oh, S. J. Kim and D. I. Cho: *9th Int. Conf. Miniaturized Systems for Chemistry and Life Sciences (Boston, 2005)* p. 1177.
- 5 D. Maillefer, H. Van Lintel, G. Rey-Mermet and R. Hirschi: *12th IEEE MEMS Conf. (Orlando, 1999)* p. 541.
- 6 S. Shoji, S. Nakagawa and M. Esashi: *Sens. Actuators A* **21** (1990) 189.
- 7 Y. H. Choi, S. U. Son and S. S. Lee: *Sens. and Actuators A* **111** (2004) 8.
- 8 W. Y. Sim, H. J. Yoon, O. C. Jeong and S. S. Yang: *J. Micromech. Microeng.* **13** (2003) 286.

- 9 K. S. Yun, I. J. Cho, J. U. Bu, C. J. Kim and E. Yoon: *J. MEMS* **11** (2002) 454.
- 10 A. B. Frazier, B. K. Gale and I. Papautsky: *Proc. 8th IEEE Int. Symp. Micromechatronics and Human Science (Nagoya, 1997)* p. 5.
- 11 L. Lin and A. P. Pisano: *IEEE/ASME J. MEMS* **8** (1999) 78.
- 12 C. C. Hong, S. Murugesan, S. H. Kim, G. Beaucage, J. W. Choi and C. H. Ahn: *Lab on a Chip* **3** (2003) 281.
- 13 M. T. Tabka, J. M. Chenal and J. M. Widmaier: *Polymer Int.* **49** (2000) 412.
- 14 R. E. Morris, A. E. Mera and R. F. Brady, Jr.: *Fuel* **79** (2000) 1101.
- 15 S. Rignuelle, C. Dubois and R. Stowe: *Propellants, Explos. Pyrotech.* **26** (2001) 118.
- 16 C. Kittel: *Introduction to Solid State Physics* (John Wiley and Sons, New York, 1996) p. 159.
- 17 S. W. Byun, J. M. Lim, S. J. Paik, A. R. Lee, K. I. Koo, S. K. Park, J. H. Park, B. D. Choi, J. M. Seo, K. A. Kim, H. Chung, S. Y. Song, D. Y. Jeon, S. S. Lee and D. I. Cho: *J. Micromech. Microeng.* **15** (2005) 1279.
- 18 M. J. de Boer, R. E. Tjerkstra, J. W. Berenschot, H. V. Jansen, G. J. Burger, J. G. E. Gardeniers, M. Elwenspoek and A. van den Berg: *IEEE/ASME J. MEMS* **9** (2000) 94.
- 19 S. J. Paik, J. T. Kim, S. J. Park, S. T. Kim, K. J. Chun, J. K. Chang and D. I. Cho: *Int. Sensor Conf. (Korea, 2001)* p. 97.
- 20 S. J. Paik, J. T. Kim, S. J. Park, S. T. Kim, K. J. Chun, J. K. Chang and D. I. Cho: *Proc. Pacific Rim Workshop on Transducers and Micro/Nano Technologies (Xiamen, 2002)* p. 725.
- 21 J. Chen and K. D. Wise: *IEEE Trans. Biomed. Eng.* **44** (1997) 760.
- 22 K. L. Zhang, S. K. Chou and S. S. Ang: *Int. J. Thermal Sci.* **10** (2006) 1016.
- 23 K. I. Koo, M. J. Jeong, S. K. Park, H. M. Choi, G. S. Kim and D. I. Cho: *World Cong. Medical Phys. and BioMedical Eng. (Seoul, 2006)* p. 306.